Available online at www.sciencedirect.com
SCIENCE DIRECT®
Nuclear Instruments and Methods in Physics Research A 556 (2006) 410–420
NUCLEAR INSTRUMENTS & METHODS IN PHYSICS RESEARCH Section A
www.elsevier.com/locate/nima

A highly polarized hydrogen/deuterium internal gas target embedded in a toroidal magnetic spectrometer

D. Cheever, E. Ihloff, J. Kelsey, H. Kolster, N. Meitanis, R. Milner, A. Shinozaki, E. Tsentalovich*, T. Zwart, V. Ziskin, Y. Xiao, C. Zhang

MIT-Bates Linear Accelerator Center, Laboratory for Nuclear Science, 21 Manning Road, Middleton, MA 01949, USA

Received 22 September 2005; received in revised form 24 October 2005; accepted 25 October 2005
Available online 18 November 2005

Abstract

A polarized hydrogen/deuterium internal gas target has been constructed and operated at the internal target region of the South Hall Ring (SHR) of the MIT-Bates Linear Accelerator Center to carry out measurements of spin-dependent electron scattering at 850 MeV. The target used an Atomic Beam Source (ABS) to inject a flux of highly polarized atoms into a thin-walled, coated storage cell. The polarization of the electron beam was determined using a Compton laser backscattering polarimeter. The target polarization was determined using well-known nuclear reactions. The ABS and storage cell were embedded in the Bates Large Acceptance Toroidal Spectrometer (BLAST), which was used to detect scattered particles from the electron–target interactions. The target has been designed to rapidly (~8 h) switch operation from hydrogen to deuterium. Further, this target was the first to be operated inside a magnetic spectrometer in the presence of a magnetic field exceeding 2 kG. An ABS intensity 2.5×10^{16} at/s and a high polarization ($\approx 70\%$) inside the storage cell have been achieved. The details of the target design and construction are described here and the performance over an 18 month period is reported.

PACS: 29.25.Pj; 29.20.Dh; 07.77.Gx

Keywords: Polarized hydrogen target; Atomic beam source; BLAST

1. Introduction

The study of the structure of the nucleon and light nuclei with spin-dependent electron scattering continues to be a subject of intense experimental [1] and theoretical [2] interest. Recent experiments using polarization techniques have produced precision data on the elastic form factors of both the proton [3] and neutron [4] at momentum transfer $q > 1\,\mathrm{GeV}/c$ and have yielded some surprising results [5]. The BLAST experiment [6] at the MIT-Bates Linear Accelerator Center was designed to measure in a comprehensive way spin-dependent electron scattering from the proton and deuteron at low momentum transfer, i.e. $q^2 \leqslant 0.8(\mathrm{GeV}/c)^2$. The central scientific focus of BLAST included:

- The determination of the ratio of the elastic charge to magnetic form factor for both the free proton and the neutron in deuterium to search for effects of the meson cloud on nucleon structure.
- The determination of the transfer of tensor polarization T_{20} in elastic electron deuteron scattering to probe the understanding of the simplest atomic nucleus, the deuteron.
- The determination of the spin structure of the deuteron at sufficiently high initial nucleon momentum to probe the understanding of the D-state.

An essential aspect of the measurements on deuterium was the existence of a successful and well tested theoretical framework for medium energy electron scattering from deuterium [7,8]. A secondary goal of the BLAST measurements was to test this framework in new regimes, involving previously unmeasured polarization observables. BLAST

*Corresponding author. Tel.: +1 617 253 9507; fax: +1 617 253 9599.
E-mail address: evgeni@mit.edu (E. Tsentalovich).

0168-9002/$ - see front matter © 2005 Elsevier B.V. All rights reserved.
doi:10.1016/j.nima.2005.10.104

uses a stored beam of longitudinally polarized electrons incident on a polarized internal gas target in the South Hall Ring (SHR) [9]. This technique permits essentially background-free measurements with little or no dilution of the experimental signal from unpolarized nucleons in the target. In addition, the extremely low-mass target-interaction area facilitates clean detection of final state products (protons, neutrons, deuterons, pions, etc.) in coincidence with the scattered electron. These are essential for the extraction of important polarization observables as a function of kinematic variables.

To carry out the BLAST scientific program, a polarized hydrogen and deuterium target was constructed and installed in early 2003. The target was commissioned in that year and production data were taken from November 2003 to May 2005. In this paper we describe the design and operating characteristics of the BLAST polarized hydrogen and deuterium target in detail.

2. Experimental setup

The MIT-Bates accelerator complex includes a polarized electron source followed by a linear accelerator with a recirculator and 1 GeV storage ring (Fig. 1). The polarized source [10] uses a strained GaAs cathode with high-gradient doping [11]. For the storage ring mode it produces electron beam pulses with a current of about 5 mA, a temporal width of 2 μs and a repetition rate of 10–20 Hz. The electrons are accelerated in the accelerator–recirculator complex to 850 MeV and then injected into the SHR. The injection takes about 30 s, and the injected current is up to 225 mA. The beam lifetime in the ring is on the order of 30 min, and when the stored current drops below a predetermined value, the injection procedure starts again. A Siberian Snake built in the Budker Institute for Nuclear Physics (Novosibirsk) [12] was installed in the ring. It keeps the longitudinal orientation of beam polarization in the internal target area. The beam polarization was constantly monitored by a Compton polarimeter [13], and an average polarization of 67% was measured. The BLAST, an open geometry spectrometer with a toroidal magnetic field, was used to detect scattered electrons and secondary particles in coincidence.

Internal gas targets are commonly used in conjunction with storage rings, where they allow for a variety of polarized and unpolarized atomic species to be used as targets for nuclear and particle physics experiments [14–16]. In an internal target, the gas atoms are injected into a T-shaped target cell where the stored beam interacts with the target gas. The gas is confined by the target cell to the region close to the beam axis, resulting in an increase of the target areal density by about two orders of magnitude over a free jet [17]. Once the gas atoms leave the target cell, they are removed from the ring vacuum pipe by means of a differential pumping system. The design goal is to remove the gas over a distance as short as possible, as the gas load affects the beam lifetime. Other design constraints include minimizing material between the target and spectrometer, ultra-high vacuum compatibility, and considerations regarding the impact on the stored beam. The BLAST polarized hydrogen/deuterium target was designed for maximum polarization and target thickness, subject to the following constraints:

- The ABS had to be located inside the BLAST magnetic toroid within an approximately cylindrical volume of

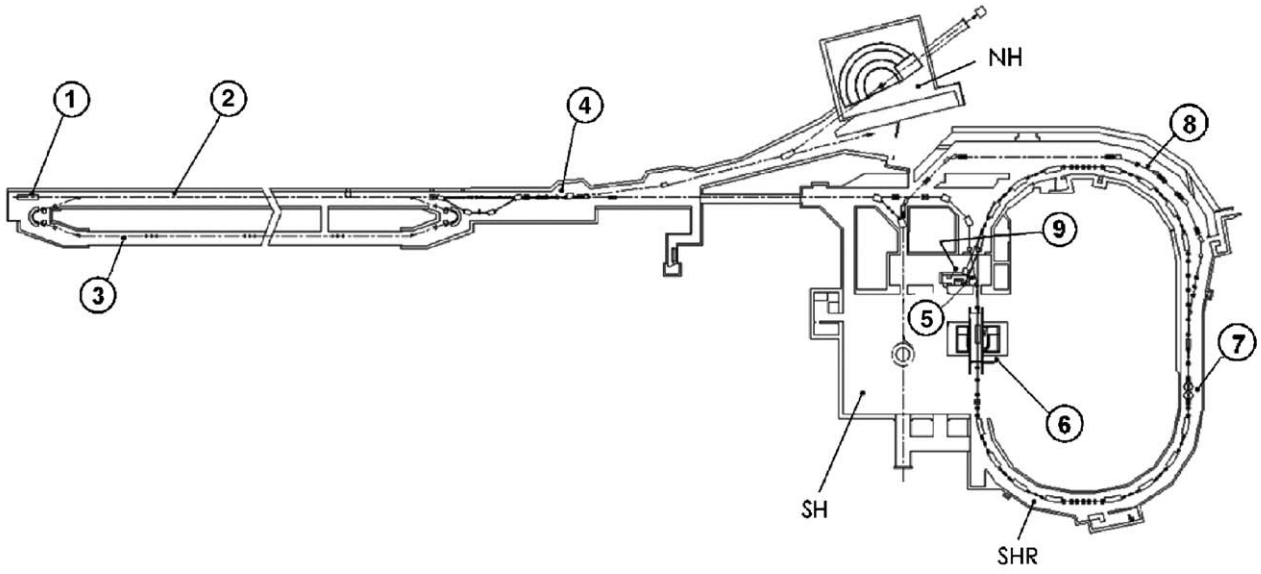

Fig. 1. MIT-Bates facility. 1—polarized electron source, 2—accelerator, 3—recirculator, 4—beam switch yard, 5—injection into SHR, 6—BLAST detector, 7—Siberian snake, 8—extraction line for experiments with external target (detectors OHIPS, OOPS), 9—Compton polarimeter, NH—North experimental Hall (SAMPLE experiment), SH—South experimental Hall.

about 1 m in diameter. Thus, the dissociator, focusing sextupole magnets, vacuum pumping and diagnostic instrumentation were located in a region of high magnetic field. The BLAST magnetic field was almost zero along the axis of the toroid (storage cell location) and it increased gradually to reach the maximum of about 2.2 kG at the location of the first sextupole magnet and then slowly decreased.

- The drifilm coated target cell was protected from the effects of beam generated radiation by a thick tungsten collimator. This maintained the target polarization at a high value over months of data taking.
- The target operation was required to be rapidly (in about 8 h) changed from hydrogen to deuterium and vice versa.
- The polarized deuterium operation required rapid (~ seconds) switching between different vector and tensor states.
- The target polarization direction was in the horizontal plane.

The ABS produces a jet of polarized atoms and injects it into the T-shaped storage cell (60 cm length, 15 mm diameter) cooled to about 100 K. A small outlet allowed some fraction of the jet to pass through the cell for polarization analysis in the Breit-Rabi Polarimeter (BRP). The holding field magnet produced the magnetic field $B_{\text{hold}} \sim 500$ G in the storage cell area that defines the orientation of target polarization. During the experiment, scattering from the target gas usually reduced the stored beam lifetime by 10–15%.

3. The atomic beam source

The ABS was originally designed and built at NIKHEF (Amsterdam) [18,19], and was shipped to Bates after AmPs finished operating. However, most of the ABS components had to be redesigned due to the unique environment. The ABS was located inside the BLAST magnetic spectrometer which produced severe space restrictions and the necessity to function in a strong magnetic field. The layout of the ABS is shown in Fig. 2.

The RF discharge in the dissociator dissociated hydrogen (or deuterium) molecules into atoms, and an atomic jet was formed in the nozzle. A 4.5 mm diameter skimmer was located 12 mm below the nozzle, and a 7.5 mm diameter aperture separated the skimmer chamber from the sextupole chamber.

Two sets of sextupole magnets were used to focus atoms from the hyperfine states with positive electron spin into the entrance of the storage cell and defocus atoms from the states with negative electron spin. A Medium Field Transition unit (MFT) was located between the first and the second sextupoles, while Strong and Weak Field Transition units (SFT and WFT) were located after the second sextupole.

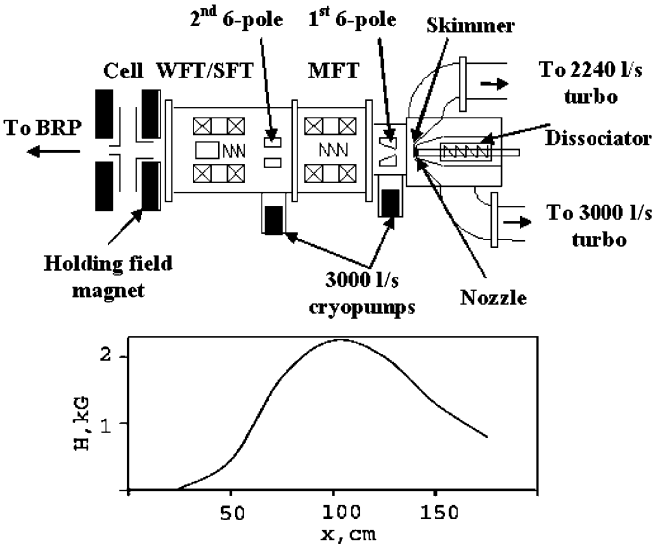

Fig. 2. Schematic layout of the ABS. The atomic beam is formed in the nozzle, two sets of sextupole magnets are focusing atoms with positive electron spin into the entrance of the storage cell; atoms with negative spin are defocused. RF transition units (MFT, SFT, WFT) are used to prepare the required vector or tensor polarization. The amplitude of the BLAST magnetic field is also shown.

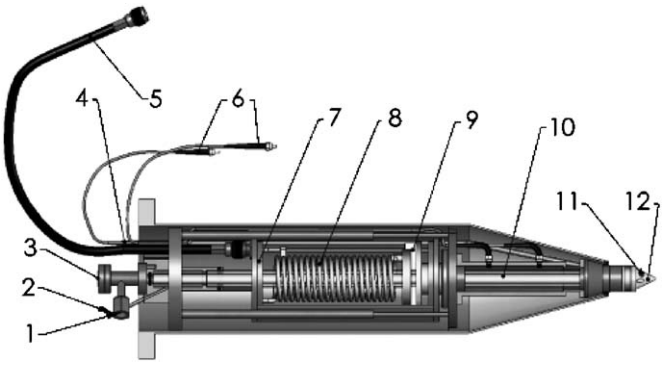

Fig. 3. Schematic layout of the dissociator. 1—hydrogen/deuterium inlet, 2—cooling water inlet, 3—viewport, 4—water outlet, 5—RF input, 6—fiber optic plasma monitors, 7—RF tank, 8—RF coil, 9—tuning plate capacitor, 10—plasma tube, 11—CERNOX temperature sensor, 12—nozzle.

3.1. Dissociator

The molecular hydrogen or deuterium gas was flown through a 9 mm inner diameter pyrex tube at a rate of ~1 mbar l/ sec (Fig. 3). A 27.1 MHz RF discharge was produced using a water-cooled solenoid. The impedance matching was achieved by remotely adjustable capacitors and monitored by an RF probe. Typically, the forward RF power was about 150 W, and the reflected power was 3–4 W. The dissociator was cooled by water. In early tests it was tried to reduce the water temperature by addition of ethylene glycol into the water. Apparently, molecules of ethylene glycol get dissociated by the RF, and the residuals covered the external surface of the dissociator, which affected the quality of the discharge. With a flux of 5 l/min

of pure de-ionized water at 10 °C, a high degree of dissociation (>90%) has been routinely achieved.

The aluminum nozzle was 2.1 mm in diameter and was attached to the end of the dissociator tube with a Teflon washer. The nozzle was cooled to about 70 K. The section of the dissociator tube near the nozzle did not have water cooling in order to avoid freezing. This section was connected to the nozzle with carefully designed copper fingers in order to keep this area cold enough to minimize recombination, and yet to exclude the freezing of the water in the dissociator.

A small ~0.001 mbar l/ sec fraction of oxygen was added to the molecular flow. In the discharge, hydrogen and oxygen atoms combined to form molecules of water. A thin ice layer covering the surface of the nozzle improved the degree of dissociation significantly. It usually took 1–2 h to create the desired layer on a fresh nozzle. After about 1 week of operation the accumulated ice became so thick that it blocked the nozzle opening and the nozzle needed to be warmed to room temperature and refreezed again. The entire procedure took about 5–7 h.

The discharge for deuterium sputtered the glass more severely than for hydrogen. As a result, a white residue accumulated on the internal surface of the nozzle, eventually reducing the degree of dissociation. The nozzle was replaced every 3 weeks during the deuterium runs, and the procedure (including nozzle realignment) took about 24 h. The hydrogen target was operated for 2 months without replacing the nozzle.

The RF coil covered only a fraction of the dissociator tube, leaving a significant area between the coil and the nozzle uncovered. However, it was found that the discharge had to extend almost to the nozzle to keep a high degree of dissociation. In order to control the discharge area, two optical sensors have been placed outside the pyrex tube: one at the middle of the RF coil, and one close to the nozzle. It was found that the BLAST magnetic field does not affect the discharge inside the coil, but it did extinguish the discharge near the nozzle, and the degree of dissociation was reduced. Magnetic shielding of the dissociator eliminated this effect.

The dissociator–nozzle assembly was installed on the mounting flange with O-ring sealing, which allowed one to adjust the nozzle location in all three dimensions. While the distance between the nozzle and the skimmer has been optimized only once, the ABS intensity was very sensitive to the transverse location of the nozzle respect to the beam axis. The procedure of the nozzle adjustment was performed every time a new nozzle was installed. A rough adjustment was made optically during the installation, while the fine adjustment—by monitoring the ABS intensity with a nozzle cooled to the operating temperature (cooling down the nozzle may produce some transverse shifts).

Cooling of the nozzle was provided by a He refrigerator with a cooling power of about 40 W, connected to the nozzle by a flexible copper braid to reduce possible shifts during the cooling down. Temperature sensors were installed on the refrigerator head, the braid and the nozzle, and a 50 W heater installed on the nozzle was used to control the nozzle temperature.

3.2. Sextupole magnets

Two sets of permanent sextupole magnets (Fig. 4) were used in the ABS. The location and profile of the magnets has been chosen according to the results of Monte Carlo simulations in order to maximize the transmission of the atoms with electron spin $+\frac{1}{2}$ and to minimize it for the atoms with spin $-\frac{1}{2}$. Fig. 5 shows the trajectories of the atoms passing through the focusing system. The transport efficiency ε is defined as a ratio of the number of atoms reaching the storage cell to the number of atoms entering the first sextupole. According to the simulation, $\varepsilon \approx 50\%$ for the spin $+\frac{1}{2}$ atoms, and $\varepsilon \approx 4\%$ for the atoms that experienced a transition in the MFT unit (i.e. atoms with spin $+\frac{1}{2}$ in the first sextupole and spin $-\frac{1}{2}$ in the second sextupole). The transport efficiency for atoms with spin $-\frac{1}{2}$ in the first sextupole is negligible. Both sextupole magnet units consist of several individual magnets with a gap in between in order to improve the pumping conductance and to minimize pressure bump formation inside the magnet units. The permanent magnets were made of VACOMAX 225 HR. This material has a somewhat lower (1.1 T) remanence than materials of VACODYM series (~1.3 T), but it has high critical temperature, which was important since originally NEG pumps were used in the sextupole chamber. The pole tip field (outside the magnet case) was about 12 kG. The sextupole magnets were mounted on retractable frames and could be moved out of the jet path via pneumatically activated linear feedthroughs.

The presence of the BLAST magnetic field was observed to produce a significant effect on the focusing in the sextupoles. Although the BLAST field was rather uniform, and it did not change the amplitude or direction of the

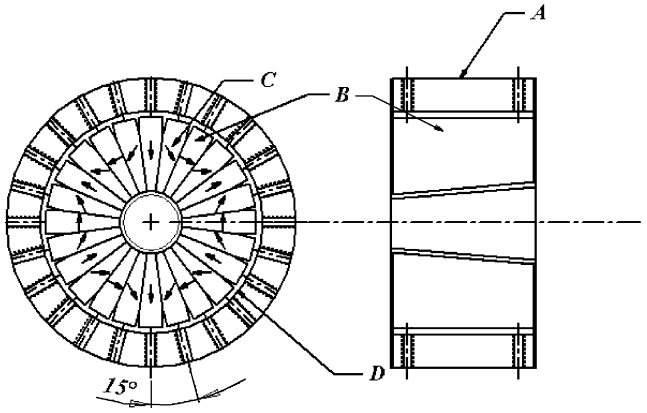

Fig. 4. One of the permanent magnet units. The magnet consists of 24 permanent magnet plates (B) with a direction of magnetization (C) rotated by 30° from plate to plate. D—epoxy, A—magnetic shielding.

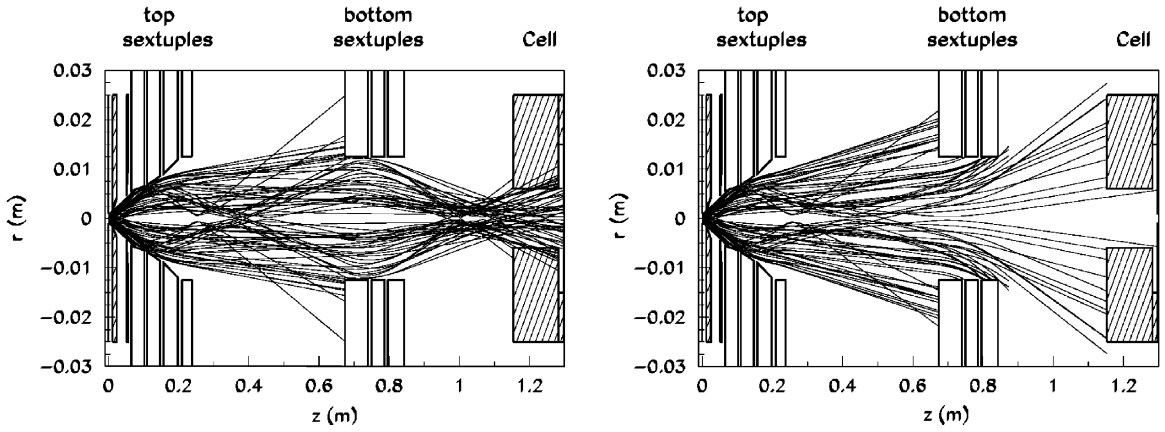

Fig. 5. Ray tracing in the ABS for atoms with electron spin $+\frac{1}{2}$ (left) and for atoms with electron spin $+\frac{1}{2}$ which experienced spin-flip in the MFT between the first and second sextupole magnets (right).

gradients in sextupole magnets, it changed the direction of the total magnetic field. The magnetic moments of the atoms follow the magnetic field adiabatically, and their direction relative to the direction of the gradient changed. Generally, the force acting on the magnetic dipole is $\vec{F} = \vec{\nabla} \cdot (\vec{\mu} \cdot \vec{B})$, and since dipoles follow the direction of the magnetic field $\vec{\mu} = \mu \cdot \vec{B}/B$, it could be transformed to $\vec{F} = \mu \cdot \vec{\nabla} B$. In an ideal sextupole ($B_x = G(x^2 - y^2)$; $B_y = -G \cdot 2xy$) with no external field the force has only a radial component:

$$\vec{F} = 2G\mu\vec{r}; \quad \frac{\vec{F}}{F} \cdot \frac{\vec{r}}{r} = 1.$$

An external magnetic field B_0 applied in the x-direction (so now $B_x = G(x^2 - y^2) + B_0$) does not affect the amplitude of the force, but it does change its direction:

$$\frac{\vec{F}}{F} \cdot \frac{\vec{r}}{r} = \frac{1 + b \cdot \cos(2\theta)}{\sqrt{1 + b^2 + 2b \cdot \cos(2\theta)}}$$

where b is a ratio of external field and sextupole field at the given point $b = B_0/B_6$ and θ is a polar angle. One can see that in the regions where the external field exceeds the sextupole field, the y-component of the force changes sign and becomes defocusing! Since the BLAST field strength was over 2 kG, and the sextupole field vanishes at the center of the sextupoles, and was about 10 kG at the pole tip, the effect was very significant and reduced the ABS intensity by factor of 2. To minimize the effect, the sextupoles were encased in magnetic shields. The ABS intensity loss was reduced to less than 10%.

3.3. RF transition units

The energy levels of the hyperfine hydrogen and deuterium states are shown in Fig. 6. In hydrogen, only atoms in states $|1>$ and $|2>$ pass the first sextupole magnet. The MFT unit induces the $2 \to 3$ transition, and only atoms in state $|1>$ pass the second sextupole. The WFT unit, located after the second sextupole, could be used to induce the $1 \to 3$ transition, effectively changing the sign of the vector polarization. For calibration purposes, the MFT may be used for the cascade $2 \to 3$; $1 \to 2$ transition, leaving only atoms in state $|2>$ after the second sextupole. This mode was used for precise identification of WFT transitions.

Similarly, for deuterium only atoms in states $|1>$,$|2>$ and $|3>$ pass the first sextupole. The MFT unit induces either $3 \to 4$ or cascade $1 \to 4$ ($3 \to 4, 2 \to 3, 1 \to 2$) transition. The SFT unit can produce either $2 \to 6$ or $3 \to 5$ transition, and the WFT unit can be used for cascade $1, 2 \to 3, 4$ transition. The polarization schemes for hydrogen and deuterium are summarized in Tables 1 and 2.

During hydrogen operation, the target was switched between states V+ and V− every 5 min. During deuterium operation, three states (V+, V−, T−) were used, producing data for both vector and tensor polarized target.

3.3.1. MFT unit

The MFT unit (Fig. 7) produced π-transitions (time-varying magnetic field is perpendicular to the static magnetic field) in a static magnetic field of 30–40 G. Transitions $2 \to 3$ and $1 \to 2$ were used for hydrogen, transitions $3 \to 4, 2 \to 3$ and $1 \to 2$ for deuterium. In some cases several transitions were used at once, and the MFT produced resonant conditions for all of them in a correct order. Since the probability of the adiabatic transitions is inversely proportional to the field gradient, the gradient should be small enough to provide high transition efficiency at the given RF field amplitude, and yet high enough to enable all transitions in the cascade. The MFT O-shaped magnet was equipped with an additional gradient coil that could produce gradients of up to 10 G/cm. The RF coil inside the MFT magnet was powered by a generator with a matching network at the input. An RF frequency of 30 MHz was used for deuterium. A higher frequency would shift components of the cascade transitions too far apart to fit in the range of the gradient coil.

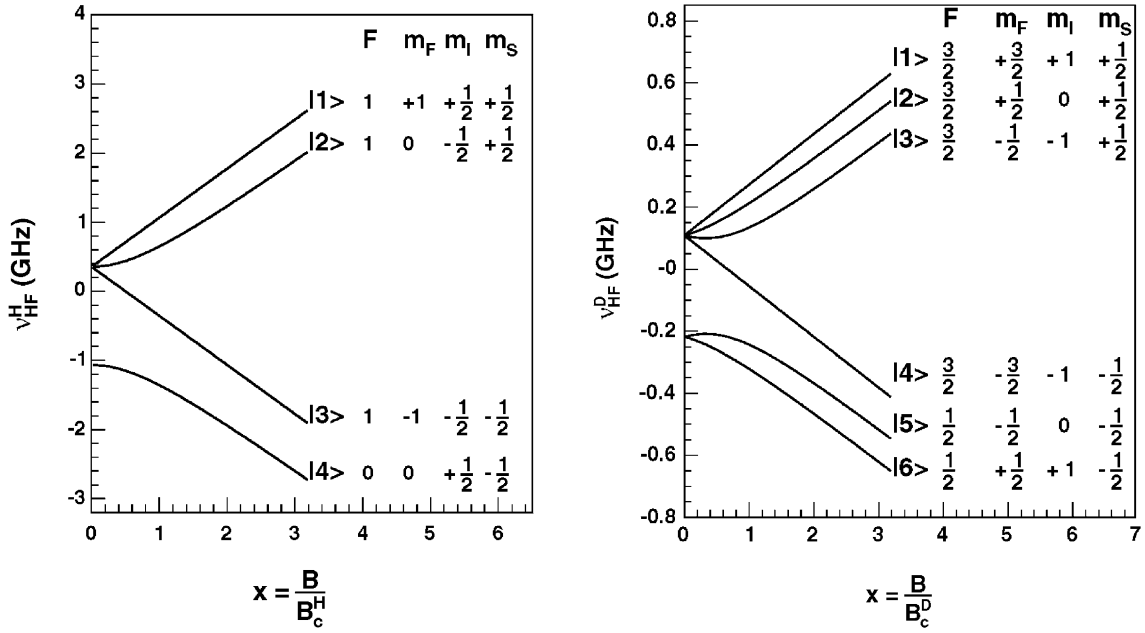

Fig. 6. Hyperfine structure of hydrogen (left) and deuterium (right) as a function of the reduced magnetic field. $B_c^{\mathrm{H}} = 507\,\mathrm{G}$; $B_c^{\mathrm{D}} = 117\,\mathrm{G}$.

Table 1
Polarization states for the hydrogen target

Name	V+	V−	Test
MFT	$2 \to 3$	$2 \to 3$	$1 \to 3$
States after sextupoles	$\|1>$	$\|1>$	$\|2>$
WFT	off	$1 \to 3$	$1 \to 3$
Final states	$\|1>$	$\|3>$	$\|2>$
P_z	+1	−1	

States marked test are used for calibration purposes only.

Table 2
Polarization states for the deuterium target

Name	V+	V−	T−	Test	Test
MFT	$3 \to 4$	$3 \to 4$	$1 \to 4$	$1 \to 4$	$2 \to 4$
States after sextupoles	$\|1>, \|2>$	$\|1>, \|2>$	$\|2>, \|3>$	$\|2>, \|3>$	$\|1>, \|3>$
WFT	off	$1,2 \to 3,4$	off	off	off
SFT	$2 \to 6$	off	$3 \to 5$	$2 \to 6$	$2 \to 6$
Final states	$\|1>, \|6>$	$\|3>, \|4>$	$\|2>, \|5>$	$\|3>, \|6>$	$\|1>, \|3>$
P_z	+1	−1	0		
P_{zz}	+1	+1	−2		

For hydrogen, with a much higher critical field, a 60 MHz frequency was used to ensure a wide enough range of the resonant conditions. End cups terminated the RF field outside in order to avoid unwanted transitions triggered by stray RF field.

The BLAST magnetic field was maximal at the location of the MFT unit, and despite heavy shielding provided by the magnet yoke, the BLAST field affected both the amplitude and the gradient of the magnetic field inside the

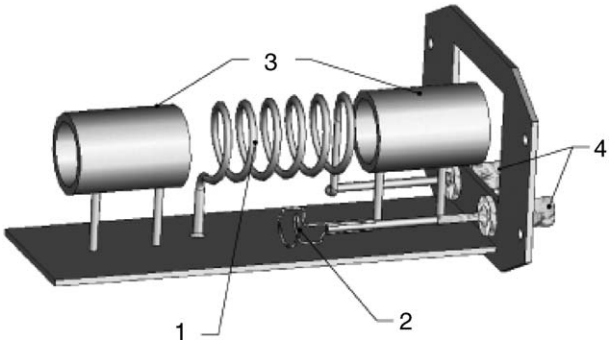

Fig. 7. Schematic layout of the MFT unit (without magnet). 1—RF coil, 2—pick-up coil, 3—RF terminators, 4—feedthrough.

MFT. The sign of the MFT static field and the direction of the gradient relative to the direction of BLAST field had to be chosen carefully. Fig. 8 shows the profile of the magnetic field in the MFT along the ABS axis. The location of resonances is shown. One can see that even if the magnetic field for a $3 \to 4$ transition involuntarily reaches the $2 \to 3$ resonance conditions, no unwanted transitions occur, since states $|2>$ and $|3>$ are equally occupied.

3.3.2. SFT and WFT units

WFT and SFT units (Fig. 9) shared the same magnet. WFT operated in a field of several Gauss. The WFT RF coil was powered by a generator similar to the one used with the MFT, with the same matching network. The working frequency was 8 MHz for deuterium, 12 MHz for hydrogen. At this location the BLAST field was rather small, but there was a strong influence of the holding field magnet. The WFT resonance conditions had to be found for every new settings of the target holding field. The SFT

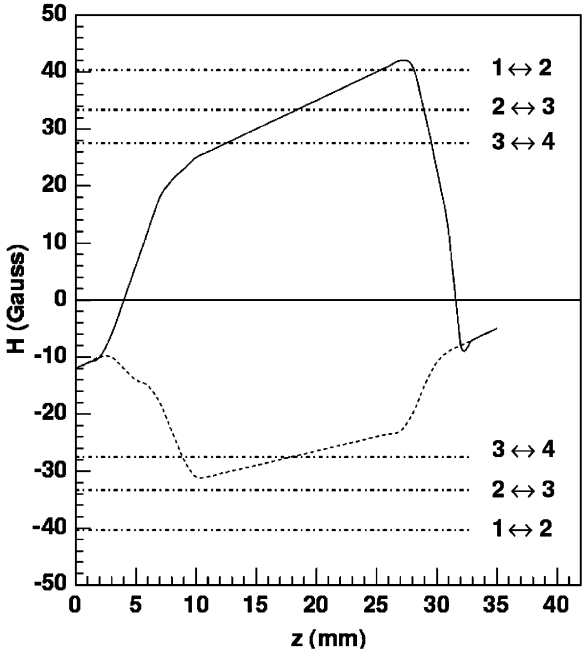

Fig. 8. Magnetic field profile (for illustration only) for MFT 1 → 4 (solid line) and MFT 3 → 4 (dashed line) transitions in deuterium.

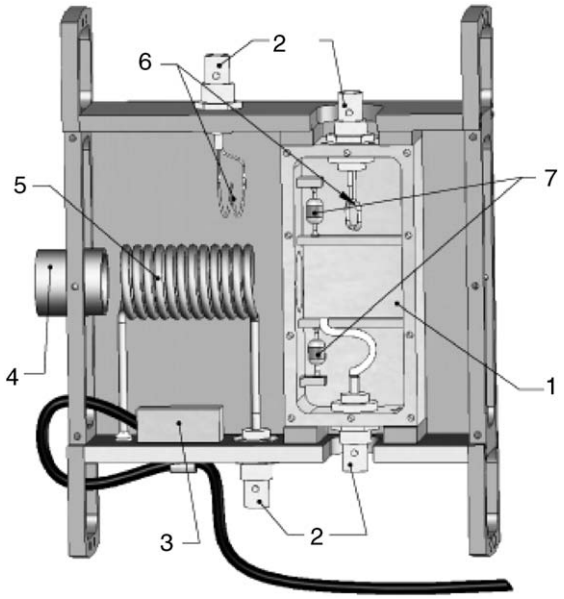

Fig. 9. Schematic layout of the SFT/WFT unit (without magnet). 1—SFT RF cavity, 2—feedthrough, 3—Hall probe, 4—RF terminator, 5—WFT RF coil, 6—pick-up coil, 7—capacitor.

unit was used for deuterium transitions only. A 420 MHz RF was fed into a rectangular cavity. The matching was achieved by adjustable capacitors built into the cavity and adjustment of the tap point. Since the SFT required significant power (forward RF power was about 10 W), semirigid cables were used inside the vacuum chamber. The surfaces of the cavity were silver-plated to reduce power losses. The magnetic field of 63 G was used for the 2 → 6 transition and 141 G for the 3 → 5 transition.

3.4. Vacuum pumping

The pumping speed is a major factor affecting ABS intensity. Fig. 10 shows a typical saturation curve as the gas flow into the dissociator increases. At a high gas flow the scattering from the residual gas in the ABS actually decreases the atomic beam intensity. There are four different vacuum chambers in the ABS: nozzle chamber, skimmer chamber, top sextupole and lower sextupole chambers. At the early stage of the ABS commissioning, the effects of the jet scattering on the residual gas were investigated by leaking additional hydrogen gas into different chambers of the ABS. The results (see Fig. 11) allowed an identification of the areas where the pumping speed improvement would make the largest impact in maximizing the ABS intensity (nozzle chamber and bottom sextupole chamber). In the final version of the target the pumping speed was increased in the first two vacuum chambers, the pump type was changed in the last two, and vacuum conductance was improved in the SFT unit. In the first two chambers the gas load was produced by the flux reflected from the skimmer and the input aperture of the sextupole chamber correspondingly. This load was rather

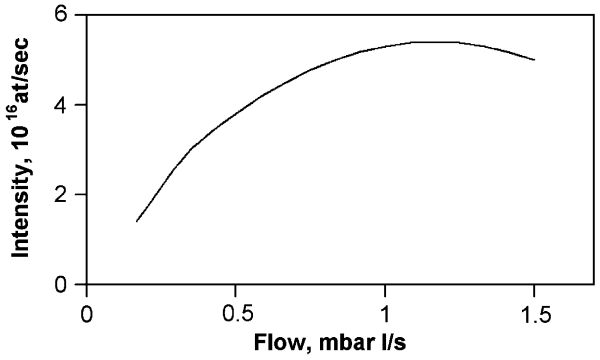

Fig. 10. ABS intensity as a function of the flow through the nozzle.

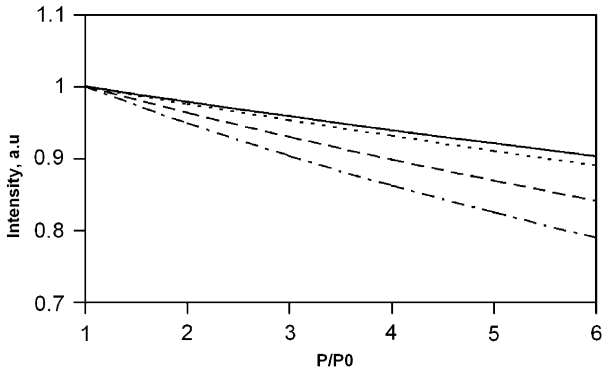

Fig. 11. ABS intensity as a function of the pressure in the different chambers. The ABS gas flow is constant and low (0.17 mbar l/s), pressure has been altered by adding gas directly into the corresponding chambers. P0—pressure in the corresponding chamber with additional flow off. Long dashed—nozzle chamber, solid—skimmer chamber, short-dashed—top sextupole chamber, dot-dashed—bottom sextupole chamber.

high: ~1 mbar l/s in the nozzle and ~0.1 mbar l/s in the skimmer chamber. Turbopumps are the pumps of choice in these conditions, but they do not operate in a large magnetic field. Four turbopumps with a total pumping speed of 5240 l/s were installed outside the magnetic field and were shielded to reduce the residual field. The pumps were connected to the ABS via long (1.5 m) pipes of a very large diameter (30 cm).

Previously the sextupole magnet chambers were pumped with two NEG pumps with pumping speed 1300 l/s each. However, the use of NEG pumps might be dangerous, since they can overheat permanent magnets during the activation. Also, it was found that they do not operate with specified pumping speed in our environment. The pumping speed degraded quickly after the activation, and the pumps saturated much faster than expected. These effects were attributed to poisoning of the NEG surfaces by non-hydrogen species originated from degassing of coils in the RF transition units. NEGs have been replaced with cryopumps of compact design and high pumping speed (3000 l/s each). It should be noted that these cryopumps broke beyond repair in a strong magnetic field (demagnetization of the valve mechanism) and required shielding to reduce the effective field below 0.5 kG.

Ion vacuum gauges also do not operate in the magnetic field, so they had to be shielded and/or moved outside the BLAST magnetic field by the means of vacuum pipe extensions.

4. Storage cell

The T-shaped storage cell was manufactured from 50 μm thick aluminum foil. The diameter of the cell was 15 mm, the length—600 mm. The inlet tube 12 mm diameter and 123 mm long was made of aluminum as well, and its conductance was equal to the half-cell conductance. Both inlet and cell were coated with drifilm to minimize wall depolarization.

The cell was suspended in the aluminum frame which was thermally insulated from the scattering chamber. A thick copper bar connected the frame to a coldhead. Circulating electron current of about 200 mA produced a significant thermal load on the cell (most likely due to wake fields), and the cell temperature was about 120–130 K during data taking.

5. Breit-Rabi polarimeter

The standard BRP with a permanent sextupole magnet, a chopping wheel and quadrupole mass analyzer (QMA) could not be used in the BLAST environment. The QMA does not work in a strong magnetic field, and it could only be used at the very bottom of the BLAST pit, some 2 m away from the target. At this distance the signal was too weak for reliable measurements. The only natural way to enhance the signal, the compression tube, has too slow a response time to be combined with a chopping wheel.

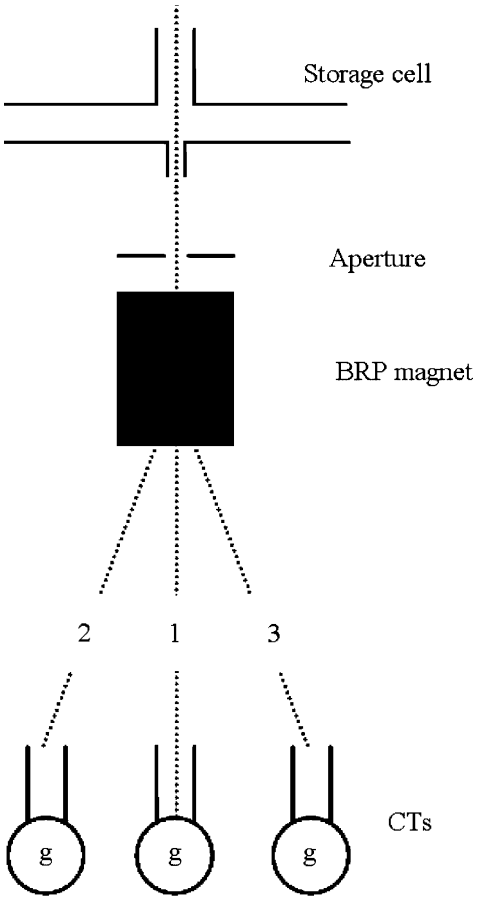

Fig. 12. BRP layout. CTs—compression tubes equipped with vacuum gauges (left, central and right). 1—trajectories of molecules, 2—trajectories of atoms with electron spin of $+\frac{1}{2}$, 3—trajectories of atoms with spin $-\frac{1}{2}$.

Instead, a BRP with a dipole magnet was used (Fig. 12). The magnet had a very strong (about 2.5 kG/cm) and uniform gradient and was placed after a small (2 mm) diaphragm below the outlet of the storage cell. Three compression tubes (CT) have been installed 1.5 m below the magnet. The compression tubes greatly enhanced the signal from the ballistic particles. The flux of 6×10^{13} at/s into the tube 75 mm long and 5 mm diameter produced a signal of about 1×10^{-6} mbar in the vacuum gauge. With a total volume of the tube and vacuum gauge of the order of 1 l, the typical response time was about 1 s.

With the dipole magnet turned off, the central CT collected both atoms and molecules. With the magnet on, the atoms were deflected into the left or right CT depending on their electron polarization. The BRP allowed measurement of both the degree of dissociation of the beam coming out of the nozzle (ABS sextupole magnets have been moved out for these measurements) and the polarization in the atomic beam. Moreover, one could monitor the polarization of the atomic beam during the production run observing the signals from the left and right CTs. Fig. 13 shows the typical signal from the CTs during the MFT scan for deuterium with SFT $2 \rightarrow 6$ transition on. One can

clearly identify the range where all three MFT transitions form a $1 \rightarrow 4$ cascade. The drawback of the system is that only the central trajectories of the atomic beam are sampled in the BRP, and therefore the absolute measurements of polarization contain significant systematic uncertainties.

6. Ion polarimeter

The ion polarimeter (Fig. 14) was designed and built at NIKHEF (Amsterdam) [20], and was implemented at Bates only partially. The electron beam ionizes atoms and molecules in the storage cell. A set of electrostatic lenses extracts the ions from the cell and accelerates them to 2.5 kV. Lenses L3, L4, L5 were split in either a vertical or horizontal direction with separate voltage control for each half for ion beam steering. A spherical deflector guided ions into the Wien filter, where they were mass analyzed. The full version included deuterium ions scattering on a tritium target to measure the polarization, but this apparatus was not installed at Bates. Even the limited version allowing to analyze the mass spectrum of the ions and therefore to measure the atomic fraction in the target proved to be very useful. In the early commissioning phase very low atomic fraction (less than 50%) in both hydrogen and deuterium targets was detected, which explained the low asymmetries measured in the scattering experiments. The cause was identified in the damage to the cell surface caused by Synchrotron Radiation (SR) and/or charge particles during the injection flash. Later the ion polarimeter was removed and a tungsten collimator was installed upstream of the storage cell. It had an internal diameter 12 mm, 3 mm smaller than that of the cell, and its shape was designed to protect the cell from the SR and charge particles and also to minimize the background rate of the detectors. With the collimator in place, the experiment took data for several months without any detectable degradation of the cell.

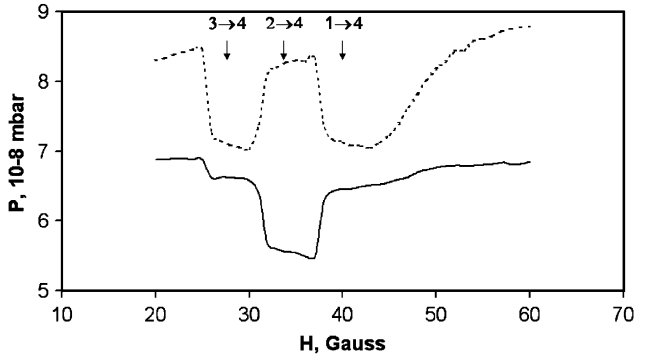

Fig. 13. MFT scan with SFT $2 \rightarrow 6$ transition on. Solid line—signal from the left CT, dashed line—from the right CT. The locations of cascade transitions are marked with the arrows.

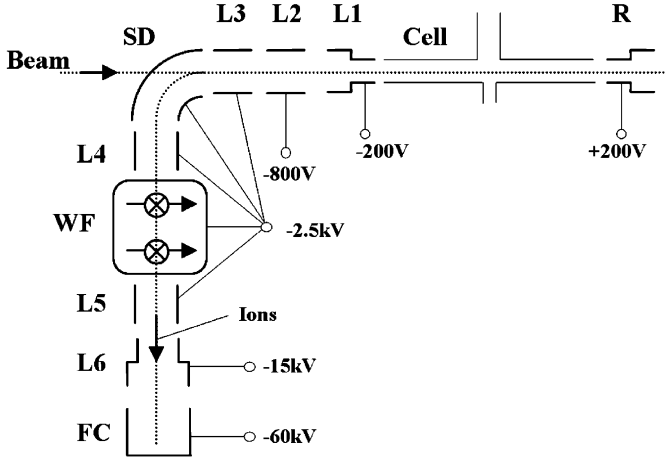

Fig. 14. Ion polarimeter. R—repeller, L1–L6—focusing and accelerating lenses, SD —spherical deflector, WF—Wien filter, FC—Faraday cup.

7. Gas feed system

The gas feed system (Fig. 15) was designed to be remotely operated and allowed for fast switching between different gases and for precise control of the gas flow. Gas bottles with hydrogen, deuterium and oxygen were connected to the manifold via remotely operated precise mass-flow controllers (MFCs) and pneumatic valves. Bypasses allowed for fast pumping of the intermediate volumes. The manifold was connected to mechanical and turbo pumps, and had an output toward the dissociator.

An unpolarized gas system which fed gas directly into the storage cell was also used for calibration purposes. It had a similar design to the polarized feed system, and allowed one to flow hydrogen, deuterium, oxygen and helium. In order to achieve a very accurate absolute calibration of the flow rate, a buffer system was built (Fig. 16). It contained two volumes of a well-known capacitance, with a remotely operated thermovalve between them. The reservoir tank was filled to a pressure of about 90 mbar, while the pressure in the buffer tank was kept constant at the desired level (usually about 2.5 mbar)

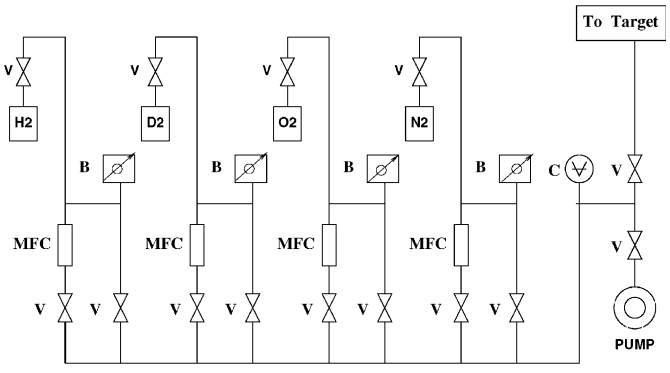

Fig. 15. Gas feed system. V—pneumatic valves, B—baratron gauges, C—convectron gauges.

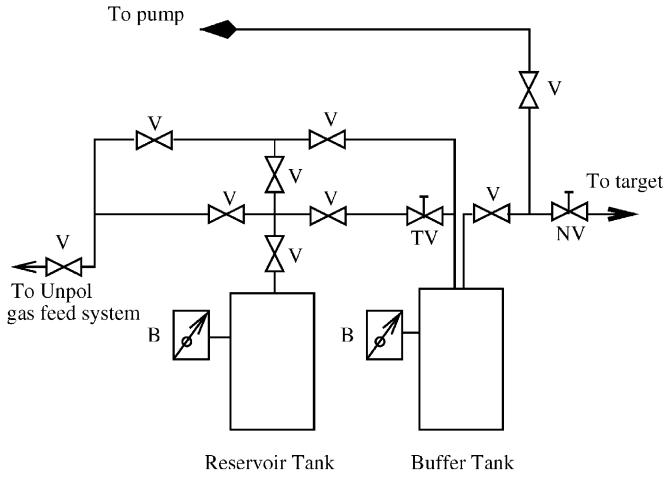

Fig. 16. Gas buffer system. TV—thermovalve, NV—needle valve.

through the thermovalve. The output from the buffer tank fed gas into the cell through the needle valve with a very stable conductance. Measurements of the pressure decrease as a function of time with the thermovalve closed allowed an accurate determination of the conductivity. Actual scattering measurements were conducted with the buffer tank pressure constant. The buffer system allowed control of the flow with an accuracy of better than 1%.

8. Control system

The Bates accelerator complex is controlled via the Experimental Physics and Industrial Control System (EPICS). All target components were integrated into this control system. Since access to the South experimental Hall where BLAST was located was very limited, all ABS components (pneumatic valves, MFCs, power supplies and RF generators, capacitors for matching networks, etc.) were remotely controlled. All sensors (Hall probes, temperature sensors, pressure gauges, etc.) were read out with a frequency of several Hz, and the updated data were transferred into the facility network, where they could be accessed by different users. All the data read from the target components were recorded on a hard drive and could be easily reviewed.

Active feedback loops were used to control the crucial components of the target. The cell temperature was affected by the electron beam (most likely due to wake fields of the electron beam). A PID controlled circuit controlled the cell temperature within several degrees. The magnetic field in the RF transition units was set with an accuracy of about 1 G to ensure resonant conditions, and the field was affected by hysteresis after the switching of the target state, or cycling of the BLAST field or holding field. The feedback loop based on the readings of the Hall probes installed inside RF transition units controlled the magnetic field with the required accuracy.

9. Target performance

Target intensity and polarization were monitored on a daily basis by measuring the rates and asymmetries of elastic and inelastic scattering (Fig. 17). For the intensity measurements the rates were compared with the same rates observed when a well-known gas flow from the unpolarized gas system was fed into the storage cell instead of ABS. Since the unpolarized gas data were taken at the same conditions as the ABS data, the systematic errors were negligible. The sudden jumps in intensity on the graph correspond to weekly maintenance procedures, which included nozzle refreezing and realignment.

Tensor polarization of deuterium target was determined by measuring elastic scattering asymmetries at low ($\sim$0.4 GeV/c) momentum transfer. The uncertainties in theoretical predictions for this momentum transfer range are small, and the systematic errors are estimated at $\sim$5%. Vector polarization of hydrogen and deuterium target was determined by measuring asymmetries in elastic p(e,e′p) and quasielastic d(e,e′p) scattering, respectively. The theoretical uncertainties for these reactions at low momentum transfer are very small and the systematic errors are less than 3%.

The ABS flow into the cell for both hydrogen (1 state) and deuterium (2 states) was about 2.5×10^{16} at/s, which produced target thickness of 7×10^{13} at/cm^2. The measured polarization of the deuterium target, averaged over

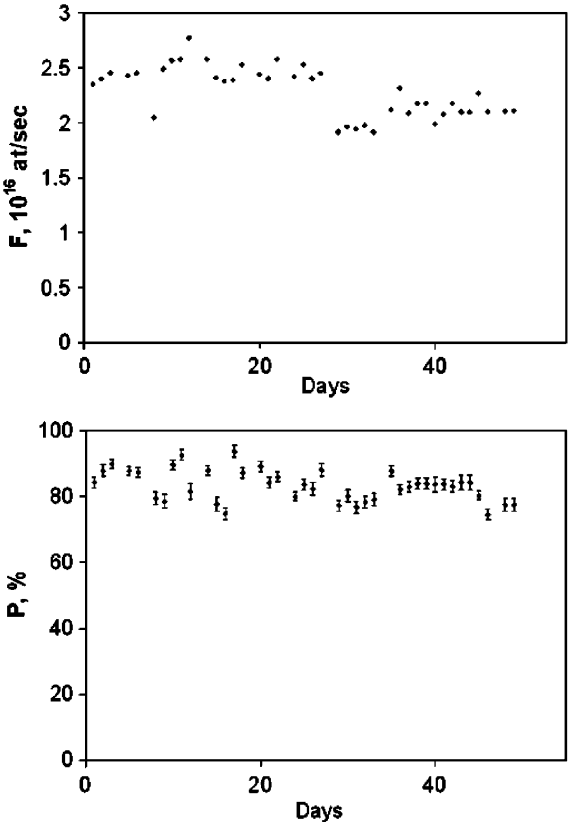

Fig. 17. ABS intensity and target polarization as a function of time during the hydrogen run.

several months of running, was $P_z \approx 86\%, P_{zz} \approx 68\%$. Polarization of the hydrogen target was $P_z \approx 82\%$.

Acknowledgements

The authors would like to thank T. Wise for his expertise in setting up cells production, Ron Holsinger and Bob Lown at Aster Enterprises, Acton, for their help in the design of the permanent magnet sextupoles. They gratefully acknowledge the help provided by Bates technicians Peter Binns, Brian O'Rourke and Steve Ciacera. They would like to thank J. van den Brand, W. Haeberli, R. Holt and Zi Lu Zhou for useful discussions.

References

[1] C. Earl Hyde-Wright, K. de Jager, Ann. Rev. Nucl. Part. Sci. 54 (2004) 217.
[2] D.R. Phillips, Phys. Lett. B 567 (2003) 12.
[3] O. Gayou, et al., Phys. Rev. Lett. 88 (2002) 092301.
[4] R. Madey, et al., Phys. Rev. Lett. 91 (2003) 122002.
[5] J. Arrington, Phys. Rev. C 71 (2005) 015202.
[6] R. Alarcon, et al., Nucl. Phys. A 663 (2000) 1111.
[7] H. Arenhovel, et al., Phys. Rev. C 46 (1992) 455.
[8] H. Arenhovel, et al., Few Body Syst. 28 (2000) 147.
[9] W.A. Franklin, et al., SPIN2004 Conference Proceeding, World Scientific, Singapore, 2004.
[10] M. Farkhondeh, et al., Proceedings of 15th International Spin Physics Symposium, Danvers, AIP, vol. 675, 2002, p. 1098.
[11] Bandwidth Semiconductor Inc., Bedford, NH.
[12] T. Zwart, et al., IEEE Proc. PAC (1995) 600.
[13] W.A. Franklin, et al., SPIN2002 Conference Proceeding AIP 675, 1058.
[14] B.B. Woitsekhovskii, et al., Izv. Akad. Nauk SSSR, Ser. Fiz. 42 (1978) 2413.
[15] R. Gilman, et al., Phys. Rev. Lett. 65 (1990) 1733.
[16] M.A. Ross, et al., Nucl. Instr. and Meth. A 344 (1994) 307.
[17] W. Haeberli, AIP Conf. Proc. 128 (1985) 251.
[18] M. Ferro-Luzzi, et al., Phys. Rev. Lett. 77 (1996) 2630.
[19] L.D. van Buuren, et al., Nucl. Instr. and Meth. A 474 (2001) 209.
[20] Z.-L. Zhou, et al., Nucl. Instr. and Meth. A 405 (1998) 165.